Hindawi Publishing Corporation
Computational and Mathematical Methods in Medicine
Volume 2017, Article ID 2729683, 16 pages
http://dx.doi.org/10.1155/2017/2729683

Research Article

Steady-State-Preserving Simulation of Genetic Regulatory Systems

Ruqiang Zhang,[1,2] Julius Osato Ehigie,[2,3] Xilin Hou,[2] Xiong You,[1] and Chunlu Yuan[1]

[1]*College of Sciences, Nanjing Agricultural University, Nanjing 210095, China*
[2]*College of Horticulture, Nanjing Agricultural University, Nanjing 210095, China*
[3]*Department of Mathematics, University of Lagos, Lagos 23401, Nigeria*

Correspondence should be addressed to Xiong You; youx@njau.edu.cn

Received 11 September 2016; Revised 11 December 2016; Accepted 18 December 2016; Published 19 January 2017

Academic Editor: Irini Doytchinova

A novel family of exponential Runge-Kutta (expRK) methods are designed incorporating the stable steady-state structure of genetic regulatory systems. A natural and convenient approach to constructing new expRK methods on the base of traditional RK methods is provided. In the numerical integration of the one-gene, two-gene, and p53-mdm2 regulatory systems, the new expRK methods are shown to be more accurate than their prototype RK methods. Moreover, for nonstiff genetic regulatory systems, the expRK methods are more efficient than some traditional exponential RK integrators in the scientific literature.

1. Introduction

One of the challenges in systems biology is to understand how biochemical molecules, such as DNAs, mRNAs, and proteins, interact to form harmonic and uniform cellular systems which give rise to life (see [1, 2]). The synthetic genetic regulatory networks (GRNs) play an important role in the investigation of protein regulation processes in living organisms (see [3–6]). By introducing ordinary differential equations (ODEs) to describe the rates of change in the concentrations of biochemical molecules, such as mRNAs and proteins, more detailed understanding and insights of the dynamic behavior exhibited by biological systems can be achieved (see [7]). The first attempt to model the oscillation in genetic regulation in terms of ODEs was made by Goodwin [8]. A standard presentation of general regulatory dynamics can be found in the monographs by Thomas and D'Ari [9] and by Fall et al. [10]. Iwamoto et al. [11] presented a dynamical model of the DNA damage signaling pathway that includes p53 and whole cell cycle regulation and explored the relationship between p53 oscillation and cell fate selection. ODEs models admit mathematically qualitative and quantitative analysis to reveal the profound properties from steady states with stability, bistability, oscillation, and limit cycles to chaos (see [12–17] and the references therein).

A typical system of ODEs governing an N-gene activation-inhibition system has the form (see Polynikis et al. [15])

$$\begin{aligned} \text{Transcription: } \dot{r}_i &= f_i^R(p) - \gamma_i r_i, \\ \text{Translation: } \dot{p}_i &= f_i^P(r_i) - \mu_i p_i, \end{aligned} \tag{1}$$

where, for $i = 1, \ldots, N$, r_i is the concentration of mRNA R_i produced by gene g_i, p_i is the concentration of protein P_i translated from mRNA R_i, γ_i is the degradation rate of R_i, and μ_i is the degradation rate of P_i. Function $f_i^P(r_i)$ is the translation function. Function $f_i^R(p)$ is the regulation function, typically taking the form of a sum of products of functions $f_{i1}^R(p_1), \ldots, f_{iN}^R(p_N)$. If protein P_j has no effect on gene g_i, $f_j^R(p_j)$ does not appear in f_i^R. The partial derivative $\partial f_i^R/\partial p_j > 0$ if protein P_j is an *activator* of gene g_i and $\partial f_i^R/\partial p_j < 0$ if protein P_j is an *inhibitor* of gene g_i. The genetic regulatory system (1) can be written in matrix form

$$\begin{aligned} \dot{r}(t) &= -\Gamma r(t) + F(p(t)), \\ \dot{p}(t) &= Kr(t) - Mp(t), \end{aligned} \tag{2}$$

where $r(t) = (r_1(t), \ldots, r_N(t))^T$ and $p(t) = (p_1(t), p_2(t), \ldots, p_N(t))^T$ are N-dimensional vectors representing the concentrations of mRNAs and proteins at time t, respectively, and $F(p(t)) = (F_1(p(t)), \ldots, F_N(p(t)))^T$, $\Gamma = \mathrm{diag}(\gamma_1, \ldots, \gamma_N)$, $M = \mathrm{diag}(\mu_1, \ldots, \mu_N)$, and $K = \mathrm{diag}(\kappa_1, \ldots, \kappa_N)$ are diagonal matrices.

The analytical solution of system (1) is in general not acquirable due to the nonlinearity of the functions $f_i^P(r_i)$ and $f_{ij}^R(p_j)$. Therefore, in order to explore the dynamics of the gene regulatory system (1), one usually resorts to numerical solution. For example, Shinto et al. [18] proposed a kinetic simulation model of metabolic pathways that describes the dynamic behaviors of metabolites in acetone-butanol-ethanol (ABE) production by *Clostridium saccharoperbutylacetonicum* N1-4 using a simulator WinBEST-KIT. So far, differential equations for genetic regulation are mostly solved by the classical four-stage Runge-Kutta (RK) method or by the Runge-Kutta-Fehlberg adaptive method (see Hairer et al. [19]). However, general-purpose RK methods have not taken into account the special structure of system (1) and fail to capture the dynamical features of the system effectively, especially in the long time simulation (see Figure 1l). Thanks to new advances in the last two decades, new approaches have been developed aiming at preserving the intrinsic geometric or physical structures of the true solution. A comprehensive account of structure-preserving algorithms can be found in the monographs by Stuart and Humphries [20], Hairer et al. [21], and Wu et al. [22]. Recently Hochbruck and Ostermann [23] investigated exponential Runge-Kutta methods for initial value problems of parabolic differential equations. This type of methods simulates exactly the linear structure of the differential equations. Defterli et al. [24] and Weber et al. [25] considered discretizing and optimizing the so-called gene-environment networks based on usually finite data series.

From the dynamics point of view, there are two basic categories of genetic regulatory systems: Category 1 consists of systems having sustained oscillation, such as limit cycles; Category 2 consists of systems having steady states. For the genetic regulatory system (1) with a limit-cycle structure, You [26] proposed a new class of phase-fitted and amplification-fitted Runge-Kutta type methods which were shown to be more effective and more efficient than the traditional Runge-Kutta methods of the same order. Very recently, You et al. [27] developed a splitting approach for genetic regulatory systems with a stable steady state. In the numerical simulation, the new splitting methods constructed in that paper are shown to be remarkably more effective and more suitable for long-term computation with large steps than the general-purpose Runge-Kutta methods. In order to respect the oscillatory feature of the solution of some genetic regulatory systems, Chen et al. [28] developed a new type of exponentially fitted TDRK (EFTDRK) methods. Zhang et al. [29] constructed a family of phase-fitted symmetric splitting methods of order two and order four. The result of the numerical experiment on the Lotka–Volterra system shows that the new phase-fitted symmetric splitting methods are more effective than their prototype splitting methods and can preserve the invariant of the system in the long term compared with the classical Runge-Kutta method of order four.

The purpose of this paper is to develop a novel type of exponential RK methods for the simulation of genetic regulatory systems which have an asymptotically stable steady state. In Section 2 we present the general scheme of exponential Runge-Kutta (expRK) methods for solving initial value problems of ODEs based on a matrix form of the variation-of-constants formula. A convenient approach of transiting traditional RK methods into a special type of expRK methods is given. In Section 3 we integrate the above three regulatory systems by the new expRK methods as well as their prototype RK methods for comparison. Section 4 is devoted to conclusive remarks. In Appendix, we analyze the linear stability and phase properties of the expRK methods.

2. Exponential Runge-Kutta Methods

2.1. Formulation of Exponential RK Methods for Systems with a Stable Steady-State Structure. Prior to dealing with the genetic regulatory system (2) numerically, we first consider the general initial value problem (IVP) of the autonomous system of ODEs

$$\begin{aligned} \dot{y} &= f(y), \quad t > 0, \\ y(0) &= y_0, \end{aligned} \tag{3}$$

where $y : [0, +\infty) \to \mathbb{R}^d$ and "$\dot{y}$" represents the derivative of y with respect to time. We make the following assumptions on system (3):

(**A1**) The origin $y^* = 0$ is a steady state of the system; that is, $f(0) = 0$.

(**A2**) The Jacobian $(\partial f/\partial y)(0)$ has eigenvalues of negative real parts in a neighborhood of the origin. Then, according to the theorem in Section 8.5 of Hirsch et al. [30], the origin is an asymptotically stable steady state; that is, for every solution $y(t)$ of system (3) through a point in the neighborhood of the steady state, $\lim_{t\to+\infty} y(t) = 0$.

(**A3**) The function $f : \mathbb{R}^d \to \mathbb{R}^d$ is continuously differentiable and satisfies the Lipschitz condition; that is, there exists a constant L (called the *Lipschitz constant*) such that

$$\|f(y) - f(z)\| \le L\|y - z\| \tag{4}$$

for all $y, z \in \mathbb{R}^d$.

Let us recall the general-purpose Runge-Kutta methods for IVP (3).

Definition 1. An s-stage Runge-Kutta (RK) method for system (3) has the scheme

$$\begin{aligned} Y_i &= y_n + h\sum_{j=1}^{s} a_{ij} f\left(Y_j\right), \quad i = 1, \ldots, s, \\ y_{n+1} &= y_n + h\sum_{i=1}^{s} b_i f\left(Y_i\right), \end{aligned} \tag{5}$$

where c_i, a_{ij}, b_i, $i, j = 1, \ldots, s$, are real numbers.

Scheme (5) can be expressed briefly by the Butcher tableau of its coefficients

$$\begin{array}{c|c} c & A \\ \hline & b^T \end{array} = \begin{array}{c|ccc} c_1 & a_{11} & \cdots & a_{1s} \\ \vdots & \vdots & \ddots & \vdots \\ c_s & a_{s1} & \cdots & a_{ss} \\ \hline & b_1 & \cdots & b_s \end{array}. \tag{6}$$

The order conditions for the RK method (5) can be found in Hairer et al. [19]. Note that the general RK scheme (5) does not take into account the special structure of the equilibrium structure of the system so that the computational results are usually not satisfactory. In order to simulate more effectively system (3) with a steady state at the origin, we rewrite problem (3) in an equivalent form

$$\begin{aligned} \dot{y} - \Omega y &= g(y), \\ y(0) &= y_0, \end{aligned} \tag{7}$$

where the matrix $\Omega = (\partial f/\partial y)(0)$, the function $g(y) = f(y) - \Omega y = \mathcal{O}(\|y\|^2)$, $\|\cdot\|$ is the Euclidean norm, and Ω is called the *rate matrix* of system (3). The matrix form of the variation-of-constants formula for system (3) is given by

$$\begin{aligned} &y(t_n + \mu h) \\ &= \exp(\mu h\Omega)\, y(t_n) \\ &\quad + \exp(\mu h\Omega) \int_{t_n}^{t_n+\mu h} \exp(-(\xi - t_n)\Omega)\, g(y(\xi))\, d\xi, \end{aligned} \tag{8}$$

where μ and h are real numbers and $t_n = nh$, $n = 0, 1, \ldots$. Approximating the integral on the right-hand side of (8) by some effective quadrature formulas leads to a numerical integrator. In general we have the following definition of the so-called exponential Runge-Kutta methods.

Definition 2. An s-stage exponential Runge-Kutta method for system (3) has the scheme

$$\begin{aligned} Y_i &= \exp(c_i V)\, y_n + \sum_{j=1}^{s} a_{ij}(V)\left(hf\left(Y_j\right) - VY_j\right), \\ &\qquad i = 1, \ldots, s, \\ y_{n+1} &= \exp(V)\, y_n + \sum_{i=1}^{s} b_i(V)\left(hf\left(Y_i\right) - VY_i\right), \end{aligned} \tag{9}$$

where c_i, $i = 1, \ldots, s$, are real numbers and $a_{ij}(V)$ and $b_i(V)$, $i, j = 1, \ldots, s$, are real $d \times d$ matrix-valued functions of matrix $V = h\Omega$.

It is convenient to express scheme (9) by the Butcher tableau

$$\begin{array}{c|c|c} c & \exp(cV) & A(V) \\ \hline & \exp(V) & b^T(V) \end{array} = \begin{array}{c|c|ccc} c_1 & \exp(c_1 V) & a_{11}(V) & \cdots & a_{11}(V) \\ \vdots & \vdots & \vdots & \ddots & \vdots \\ c_s & \exp(c_1 V) & a_{s1}(V) & \cdots & a_{ss}(V) \\ \hline & \exp(V) & b_1(V) & \cdots & b_s(V) \end{array}, \tag{10}$$

where $\exp(cV) = (\exp(c_1 V)^T, \ldots, \exp(c_s V)^T)^T$. For a comprehensive review of exponential integrators with the construction, analysis of convergence and error bounds, order conditions, example integrators, and applications, the reader is referred to Hochbruck and Ostermann [23].

It is noted that if we need to integrate a system $z' = \psi(z)$ near a stable steady state $z^* \neq 0$, the exponential RK scheme (9) should take the form

$$\begin{aligned} y_n &= z_n - z^*, \\ Y_i &= \exp(c_i V)\, y_n \\ &\quad + \sum_{j=1}^{s} a_{ij}(V)\left(h\psi\left(Y_j + z^*\right) - VY_j\right), \\ &\qquad i = 1, \ldots, s, \\ y_{n+1} &= \exp(V)\, y_n + \sum_{i=1}^{s} b_i(V)\left(h\psi\left(Y_i + z^*\right) - VY_i\right), \\ z_{n+1} &= y_{n+1} + z^*, \end{aligned} \tag{11}$$

where $V = h\Omega$ with $\Omega = (\partial\psi/\partial z)(z^*)$.

2.2. A Special Class of Exponential RK Methods. Based on an RK method (5), we can formulate, as a special case of the exponential RK method (9), the following scheme for system (3):

$$\begin{aligned} Y_i &= \exp(c_i V)\, y_n \\ &\quad + \sum_{j=1}^{s} a_{ij} \exp\left(\left(c_i - c_j\right)V\right)\left(hf\left(Y_j\right) - VY_j\right), \\ &\qquad i = 1, \ldots, s, \\ y_{n+1} &= \exp(V)\, y_n \\ &\quad + \sum_{i=1}^{s} b_i \exp\left(\left(1 - c_i\right)V\right)\left(hf\left(Y_i\right) - VY_i\right), \end{aligned} \tag{12}$$

where c_i, a_{ij}, and b_i, $i, j = 1, \ldots, s$, are the constant coefficients of the RK method (5). Note that as $\Omega \to 0$ ($V \to 0$), scheme (12) reduces to the RK method (5). The latter is called the *prototype RK method* of the former. In the sequel of this paper, scheme (12) will be referred to as an *expRK method*. Its Butcher tableau can be written as follows:

$$\begin{array}{c|c|c} c & \exp(cV) & \exp(cV)^T A \exp(-cV) \\ \hline & \exp(V) & b^T \exp((e-c)V) \end{array}$$

$$= \begin{array}{c|c|ccccc} c_1 & \exp(c_1 V) & a_{11} & a_{12}\exp((c_1-c_2)V) & \cdots & a_{1s}\exp((c_1-c_s)V) \\ \vdots & \vdots & \vdots & \vdots & \ddots & \vdots \\ c_s & \exp(c_1 V) & a_{s1}\exp((c_s-c_1)V) & a_{s2}\exp((c_s-c_2)V) & \cdots & a_{ss} \\ \hline & \exp(V) & b_1\exp((1-c_1)V) & b_2\exp((1-c_2)V) & \cdots & b_s\exp((1-c_s)V) \end{array}, \tag{13}$$

where $e = (1,\ldots,1)^T$, $\exp((e-c)V = (\exp((1-c_1)V)^T,\ldots,\exp((1-c_s)V)^T)^T$, and $\exp(cV)^T A\exp(-cV) = (\exp((c_i - c_j)V)a_{ij})_{s\times s}$.

In Kronecker's notation, scheme (12) can be written as

$$\begin{aligned} Y &= \exp(cV)\, y_n \otimes e \\ &\quad + \exp(cV)\,(A\otimes I_d)\left(\exp(-cV)\,(hf(Y) - VY)\right), \\ y_{n+1} &= \exp(V)\, y_n \\ &\quad + \exp(V)\left(b^T \otimes I_d\right)\left(\exp(-cV)\,(hf(Y) - VY)\right), \end{aligned} \tag{14}$$

where I_d is the $d\times d$ unit matrix and $\exp(-cV)(hf(Y)-VY) = (\exp((-c_1)V)^T(hf(Y_1) - VY_1),\ldots,\exp((-c_s)V)^T(hf(Y_s) - VY_s))^T$.

Among simple examples are the following:

(a) The *exponential Euler method* (explicit), denoted by expEuler:

$$y_{n+1} = \exp(V)\, y_n + \exp(V)\,(hf(y_n) - Vy_n) \tag{15}$$

(b) The *exponential backward Euler method* (implicit), denoted by expImEuler:

$$y_{n+1} = \exp(V)\, y_n + (hf(y_{n+1}) - Vy_{n+1}) \tag{16}$$

(c) The *exponential trapezoidal rule* (implicit), denoted by expTrap:

$$\begin{aligned} y_{n+1} &= \exp(V)\, y_n + \frac{\exp(V)}{2}\,(hf(y_n) - Vy_n) \\ &\quad + \frac{1}{2}\,(hf(y_{n+1}) - Vy_{n+1}) \end{aligned} \tag{17}$$

(d) The *exponential Heun rule* (explicit), denoted by expHeun:

$$\begin{aligned} y_p &= \exp(V)\, y_n + \exp(V)\,(hf(y_n) - Vy_n), \\ y_c &= \exp(V)\, y_n + (hf(y_p) - Vy_p), \\ y_{n+1} &= \frac{y_p + y_c}{2} \end{aligned} \tag{18}$$

(e) The *exponential midpoint rule* (implicit), denoted by expMid:

$$\begin{aligned} y_{n+1} &= \exp(V)\, y_n + \exp\left(\frac{V}{2}\right) \\ &\quad \cdot \left(hf\left(\frac{\exp(V/2)\, y_n + \exp(-V/2)\, y_{n+1}}{2}\right)\right. \\ &\quad \left. - \frac{1}{2}V\left(\exp\left(\frac{V}{2}\right) y_n + \exp\left(-\frac{V}{2}\right) y_{n+1}\right)\right) \end{aligned} \tag{19}$$

Two typical expRK methods, denoted by expRK3/8 and expRK4, have the prototype RK methods of order four, denoted by RK3/8 and RK4, respectively, whose respective Butcher tableaux are given in Page 138 of [19]

$$\begin{array}{c|cccc} 0 & & & & \\ \frac{1}{3} & \frac{1}{3} & & & \\ \frac{2}{3} & -\frac{1}{3} & 1 & & \\ 1 & 1 & -1 & 1 & \\ \hline & \frac{1}{8} & \frac{3}{8} & \frac{3}{8} & \frac{1}{8} \end{array}, \tag{20}$$

$$\begin{array}{c|cccc} 0 & & & & \\ \frac{1}{2} & \frac{1}{2} & & & \\ \frac{1}{2} & 0 & \frac{1}{2} & & \\ 1 & 0 & 0 & 1 & \\ \hline & \frac{1}{6} & \frac{2}{6} & \frac{2}{6} & \frac{1}{6} \end{array} \tag{21}$$

The (algebraic) order is a measure of the accuracy of numerical method. A method is said to have *order p* if its local error LE = $\mathcal{O}(h^{p+1})$.

Theorem 3. *The expRK method (12) has the same algebraic order as its prototype RK method.*

Proof. The conclusion follows by expanding the exponential functions $\exp(c_i V)$, $\exp((c_i - c_j)V)$, and $\exp((1 - c_i)V)$ in scheme (12) in series of $V = h\Omega$, hence in series of h, and comparing this series with that of the true solution. □

The next theorem asserts that exponential RK method (12) preserves the steady state of system (3).

Theorem 4. *Suppose that f in system (3) satisfies the Lipschitz condition and the origin is a steady state of the system; that is, $f(0) = 0$. Then the origin is also a fixed point of the expRK method (12) for small step size h.*

The proof is given in Appendix A.

In order to apply the expRK method (9) or (12) to system (2), we first use a coordinate transform $u(t) = r(t) - r^*$, $v(t) = p(t) - p^*$ to translate the steady state (r^*, p^*) of the system to the origin and yields

$$\begin{aligned} \dot{u}(t) &= -\Gamma u(t) + F'(p^*)\, v(t) + G(v(t)), \\ \dot{v}(t) &= K u(t) - M v(t), \end{aligned} \tag{22}$$

where $F'(p^*)$ is the Jacobian matrix of $F(p)$ at point p^* and $G(v(t)) = F(p^* + v(t)) - F'(p^*)v(t) - F(p^*)$. Then system (2) can be written in the form (7) with $y(t) = (u(t), v(t))^T$ where the rate matrix

$$\Omega = \begin{pmatrix} -\Gamma & F'(p^*) \\ K & -M \end{pmatrix} \tag{23}$$

and the function $g(y) = (G(v)^T, \mathbf{0})^T$.

3. Numerical Illustrations

From Theorem 4, contrast to traditional RK methods, exponential RK methods, especially expRK methods, retain the rate of growth, phase, and amplification of the exact solution of the test equation (B.1) without error. Then it is reasonable to expect expRK (12) to be more effective than their prototype RK methods. In this section, in order to compare their effectiveness, we apply them to three test systems—one-gene self-regulation system, two-gene cross-regulation system, and the p53-mdm2 system.

(I) A One-Gene System of Self-Regulation. The first model we consider is the one-gene system with self-regulation given by

$$\begin{aligned} \dot{r}(t) &= -\gamma r(t) + F(p(t)), \\ \dot{p}(t) &= -\mu p(t) + \kappa r(t), \end{aligned} \tag{24}$$

where $F(p(t)) = \alpha/(1 + p(t)^2/\theta^2)$ represents the action of an inhibitory protein that acts as a dimer and $\gamma, \mu, \kappa, \alpha, \theta$ are positive constants. For a similar model with delays see Xiao and Cao [31].

(II) A Two-Gene System with Cross-Regulation. The second model is a two-gene activation-inhibition system with cross-regulation (studied by Polynikis et al. [15], Widder et al. [17], Chen et al. [32], You [26], and You et al. [27])

$$\begin{aligned} \dot{r}_1 &= m_1 H^+(p_2; \theta_2, n_2) - \gamma_1 r_1, \\ \dot{r}_2 &= m_2 H^-(p_1; \theta_1, n_1) - \gamma_2 r_2, \\ \dot{p}_1 &= \kappa_1 r_1 - \mu_1 p_1, \\ \dot{p}_2 &= \kappa_2 r_2 - \mu_2 p_2, \end{aligned} \tag{25}$$

where, for $i = 1, 2$, r_i is the concentration of mRNA R_i produced by gene g_i, p_i is the concentration of protein P_i, m_i is the maximal transcription rate of gene g_i, κ_i is the translation rate of mRNA R_i, and γ_i and μ_i are the degradation rates of mRNA R_i and protein P_i, respectively. The functions

$$\begin{aligned} H^+(p_2; \theta_2, n_2) &= \frac{p_2^{n_2}}{\theta_2^{n_2} + p_2^{n_2}}, \\ H^-(p_1; \theta_1, n_1) &= \frac{\theta_1^{n_1}}{\theta_1^{n_1} + p_1^{n_1}} \end{aligned} \tag{26}$$

are the *Hill functions* of activation and repression, respectively. The parameters θ_1, θ_2 are the *expression thresholds*. The integer value of n_i $(i = 1, 2)$, called the *Hill coefficient*, stands for the number of protein monomers required for saturation of binding to DNA. It is easy to see that the activation function H^+ is increasing in p_2 and the repression function H^- is decreasing in p_1.

(III) The p53-mdm2 System. The third model is for the damped oscillation of the p53-mdm2 regulatory pathway. Strictly speaking, this system is not of the form (1). We adopt this model since its solutions also have a stable steady-state structure of interest. The system, given by van Leeuwen et al. [33] with the small transient stress stimulus $S(t) = 0$, has the form

$$\begin{aligned} \dot{P}_I &= s_p + j_a P_A - d_p P_I - k_c P_I M + j_c C, \\ \dot{M} &= s_{m0} + \frac{s_{m1} P_I + s_{m2} P_A}{P_I + P_A + K_m} + (k_u + j_c) C \\ &\quad - (d_m + k_c P_I) M, \\ \dot{C} &= k_c P_I M - (j_c + k_u) C, \\ \dot{P}_A &= -(j_a + d_p) P_A, \end{aligned} \tag{27}$$

where P_I represents the concentration of the p53 tumor suppressor, M (mdm2) is the concentration of the p53's main negative regulator, C is the concentration of the p53-mdm2 complex, P_A is the concentration of an active form of p53 that is resistant against mdm2-mediated degradation, s_* $(* = p, m0, m1)$ are de novo synthesis rates, k_* $(* = a, c, u)$ are production rates, j_* $(* = a, c)$ are reverse reactions (e.g., dephosphorylation), d_p is the degradation rate of active p53, and K_m is the saturation coefficient.

3.1. Accuracy Test

3.1.1. The One-Gene System. Steady states of system (24) can be determined by the cubic equation $(1/\theta^2)p^{*3}+p^*+\alpha\kappa/\gamma\mu = 0$ and the relation $r^* = (\mu/\kappa)p^*$. If the system is written in the form (7), the rate matrix

$$\Omega = \begin{pmatrix} -\gamma & -\dfrac{2\alpha p^*/\theta^2}{\left(1+p^{*2}/\theta^2\right)^2} \\ \kappa & -\mu \end{pmatrix}, \tag{28}$$

and the function

$$g(y) = \begin{pmatrix} \dfrac{\alpha}{1+\left(y_2+p^*\right)^2/\theta^2} + \dfrac{2\alpha p^*/\theta^2}{\left(1+p^{*2}/\theta^2\right)^2} y_2 \\ 0 \end{pmatrix}, \tag{29}$$

where $y = (y_1, y_2)^T = (r - r^*, p - p^*)$. With the parameter values (provided by [31])

$$\begin{aligned} \alpha &= 3, \\ \gamma &= 1, \\ \mu &= 1.5, \\ \kappa &= 5, \\ \theta &= 1, \end{aligned} \tag{30}$$

this system has a unique positive steady state $(r^*, p^*) = (0.6, 2)$ where the rate matrix Ω has eigenvalues $\lambda_{1,2} = -1.2500 \pm 2.9767i$, where i is the imaginary unit satisfying $i^2 = -1$. Since the two eigenvalues both have negative real parts, the steady state is asymptotically stable. Figure 1(a) shows three solution trajectories on the phase plane starting at $(r(0), p(0)) = (0.2, 0.3), (0.2, 0.8), (0.2, 2.3)$, respectively. Figure 1(b) shows the time evolution of concentrations of mRNA and protein starting at $(r(0), p(0)) = (1.2, 0.3)$.

With the above values of parameters and initial data, we integrate system (25) on the time interval $[0, 100]$ by the methods expEuler, expHeun, expRK3/8, and expRK4 as well as their corresponding prototype methods. We plot the error growth of the protein on the time interval $[50, 100]$. The numerical results are presented in Figures 2 and 3.

The system is solved on the time interval $[0, 100]$ with initial values of mRNA and protein $r(0) = 0.6$ and $p(0) = 0.8$ and with different step sizes. The numerical results are presented in Tables 1 and 2.

3.1.2. The Two-Gene System. The steady states $y^* = (r_1^*, r_2^*, p_1^*, p_2^*)^T$ of system (25) are determined by the equations

$$\begin{aligned} &\theta_2^{n_2} p_1^* \left(p_1^{*n_1} + \theta_1^{n_1}\right)^{n_2} + \left(p_1^* - \frac{m_1 k_1}{\gamma_1 \mu_1}\right)\left(\frac{m_2 k_2}{\gamma_2 \mu_2}\theta_1^{n_1}\right)^{n_2} \\ &\quad = 0, \end{aligned} \tag{31}$$

$$\begin{aligned} r_1^* &= \frac{\mu_1}{\kappa_1} p_1^*, \\ r_2^* &= \frac{\mu_2}{\kappa_2} p_2^*, \\ p_2^* &= \frac{m_2 \kappa_2 \theta_1^{n_1}}{\gamma_2 \mu_2 \left(\theta_1^{n_1} + p_1^{*n_1}\right)}. \end{aligned} \tag{32}$$

Putting in the form (7), system (25) has the rate matrix

$$\begin{aligned} \Omega &= \frac{\partial f}{\partial y}(y^*) \\ &= \begin{pmatrix} -\gamma_1 & 0 & 0 & \dfrac{m_1 n_2 \theta_2^{n_2} p_2^{*n_2-1}}{\left(\theta_2^{n_2} + p_2^{*n_2}\right)^2} \\ 0 & -\gamma_2 & -\dfrac{m_2 n_1 \theta_1^{n_1} p_1^{*n_1-1}}{\left(\theta_1^{n_1} + p_1^{*n_1}\right)^2} & 0 \\ \kappa_1 & 0 & -\mu_1 & 0 \\ 0 & \kappa_2 & 0 & -\mu_2 \end{pmatrix} \end{aligned} \tag{33}$$

and the function

$$\begin{aligned} &g(y) \\ &= \begin{pmatrix} m_1 \dfrac{{p_2}^{n_2}}{\theta_2^{n_2} + \left(y_4 + p_2^*\right)^{n_2}} - \gamma_1 r_1^* - \dfrac{m_1 n_2 \theta_2^{n_2} p_2^{*n_2-1}}{\left(\theta_2^{n_2} + p_2^{*n_2}\right)^2} y_4 \\ m_2 \dfrac{\theta_1^{n_1}}{\theta_1^{n_1} + \left(y_3 + p_1^*\right)^{n_1}} - \gamma_2 r_2^* - \dfrac{m_2 n_1 \theta_1^{n_1} p_1^{*n_1-1}}{\left(\theta_1^{n_1} + p_1^{*n_1}\right)^2} y_3 \\ 0 \\ 0 \end{pmatrix} \end{aligned} \tag{34}$$

with $y = (y_1, y_2, y_3, y_4)^T = (r_1 - r_1^*, r_2 - r_2^*, p_1 - p_1^*, p_4 - p_4^*)^T$. The characteristic equation of the rate matrix Ω is

$$\left(\lambda + \gamma_1\right)\left(\lambda + \gamma_2\right)\left(\lambda + \mu_1\right)\left(\lambda + \mu_2\right) + D = 0, \tag{35}$$

where

$$D = m_1 m_2 \kappa_1 \kappa_2 \frac{n_1 n_2 p_1^{*n_1-1} p_2^{*n_2-1} \theta_1^{n_1} \theta_2^{n_2}}{\left(p_1^{*n_1} + \theta_1^{n_1}\right)^2 \left(p_2^{*n_2} + \theta_2^{n_2}\right)^2}. \tag{36}$$

For a certain value of $D = D_{\text{Hopf}}$, the real part of one of the eigenvalues crosses zero, indicating a loss of stability through a Hopf bifurcation. For $n_1 > 1$ and $n_2 > 1$, [17] has calculated this value explicitly as

$$\begin{aligned} &D_{\text{Hopf}} \\ &= \frac{\left(\gamma_1 + \gamma_2\right)\left(\gamma_1 + \mu_1\right)\left(\gamma_2 + \mu_1\right)\left(\gamma_1 + \mu_2\right)\left(\gamma_2 + \mu_2\right)\left(\mu_1 + \mu_2\right)}{\left(\gamma_1 + \gamma_2 + \mu_1 + \mu_2\right)^2}. \end{aligned} \tag{37}$$

In our experiment, we take the values of parameters as follows:

$$\begin{aligned} n_1 &= n_2 = 3, \\ m_1 &= m_2 = 1.8, \\ k_1 &= k_2 = 1, \\ \gamma_1 &= \gamma_2 = 1, \\ \mu_1 &= \mu_2 = 1, \\ \theta_1 &= \theta_2 = 0.6542. \end{aligned} \tag{38}$$

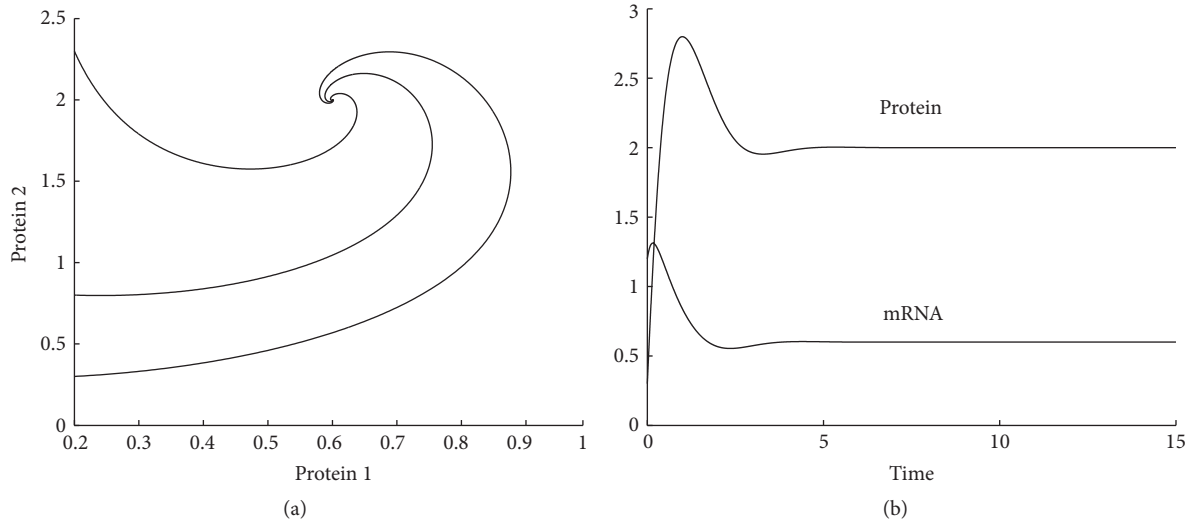

Figure 1: One-gene system: (a) solution trajectories; (b) time evolution of concentrations of mRNA and protein.

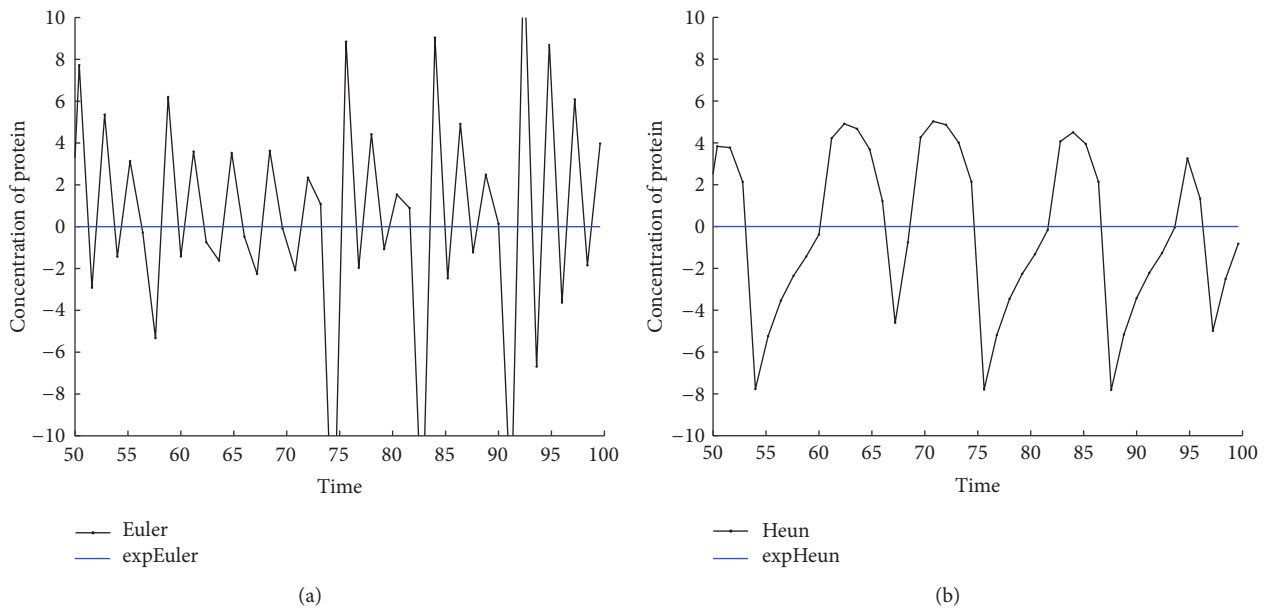

Figure 2: Accuracy comparison for the one-gene system: (a) Euler and expEuler; (b) Heun and expHeun with step size $h = 1.2$.

Figure 4(a) shows three solution trajectories projected on the mRNA 1-protein 1 plane starting at $(r_1(0), r_2(0), p_1(0), p_2(0)) = (0.1, 0.5, 0, 0)$,$(0.3, 0.3, 0, 0)$, and $(0.5, 0.2, 0, 0)$, respectively. Figure 4(b) shows the time evolution of concentrations of protein 1 and protein 2.

We solve (31) for p_1^* by Newton's iteration and then substitute it into (32) obtaining

$$\begin{aligned} r_1^* &= 0.81471271066221, \\ r_2^* &= 0.61403210214378, \\ p_1^* &= 0.81471271066221, \\ p_2^* &= 0.61403210214378. \end{aligned} \tag{39}$$

The rate matrix (33) has the eigenvalues with negative real parts:

$$\begin{aligned} \lambda_{1,2} &= -1.94911366876016 \pm 0.94911366876016i, \\ \lambda_{3,4} &= -0.05088633123984 \pm 0.94911366876016i. \end{aligned} \tag{40}$$

Therefore the steady state y^* is asymptotically stable.

With the values of parameters (38) and initial data and initial values $r_1(0) = 0.6$, $r_2(0) = 0.8$, $p_1(0) = 0$, and $p_2(0) = 0$, we integrate system (25) on the time interval $[0, 100]$ by the methods expEuler, expHeun, expRK3/8, and expRK4 as well as their corresponding prototype methods with the step sizes $h = 1.8$, $h = 1.7$, $h = 1.5$, $h = 1.678$, respectively. In Figures 5 and 6, we plot the global error growth of protein 1 on the time interval $[50, 100]$.

In Tables 3 and 4, average errors are compared for differential step sizes.

3.1.3. The p53-mdm2 System. The steady state $y^* = (P_I^*, M^*, C^*, P_A^*)$ is determined by the following equations:

$$s_p - d_p P_I^* - \frac{k_c k_u}{d_m (j_c + k_u)} P_I^* \left(s_{m0} + \frac{s_{m1}}{P_I^* + K_m} P_I^* \right) = 0,$$

$$M^* = \frac{s_{m0}}{d_m} + \frac{s_{m1} P_I^*}{d_m (P_I^* + K_m)},$$

$$C^* = \frac{k_c}{j_c + k_u} P_I^* M^*,$$

$$P_A^* = 0. \tag{41}$$

Putting in the form (7), system (27) has the rate matrix

$$\Omega = \frac{\partial f}{\partial y}(y^*) = \begin{pmatrix} -d_p - k_c M^* & -k_c P_I^* & j_c & j_a \\ \dfrac{s_{m1} K_m + (s_{m1} - s_{m2}) P_A^*}{(P_I^* + P_A^* + K_m)^2} - k_c M^* & -(d_m + k_c P_I^*) & k_u + j_c & \dfrac{s_{m2} K_m + (s_{m2} - s_{m1}) P_I^*}{(P_I^* + P_A^* + K_m)^2} \\ k_c M^* & k_c P_I^* & -(k_u + j_c) & 0 \\ 0 & 0 & 0 & j_a + d_p \end{pmatrix}. \tag{42}$$

and the function

$$g(y) = \begin{pmatrix} -k_c y_1 y_2 \\ g_2(y) \\ k_c y_1 y_2 \\ 0 \end{pmatrix}, \tag{43}$$

where $y = (y_1, y_2, y_3, y_4)^T = (P_I - P_I^*, M - M^*, C - C^*, P_A - P_A^*)^T$, and

$$g_2(y) = -\frac{(((s_{m1} - s_{m2}) P_A^* + s_{m1} K_m) y_1 + ((s_{m2} - s_{m1}) P_I^* + s_{m2} K_m) y_4)(y_1 + y_4)}{(y_1 + P_I^* + y_4 + P_A^* + K_m)(P_I^* + P_A^* + K_m)^2} - k_c y_1 y_2. \tag{44}$$

We use the parameter values (see [33]) as follows:

$$\begin{aligned} s_{m0} &= 2 \times 10^{-3}\ \text{nM min}^{-1}, \\ k_a &= 20\ \text{min}^{-1}, \\ j_a &= 0.2\ \text{min}^{-1}, \\ s_{m1} &= 0.15\ \text{nM min}^{-1}, \\ k_c &= 4\ \text{min}^{-1}\ \text{nM}^{-1}, \\ j_c &= 2 \times 10^{-3}\ \text{min}^{-1}, \\ s_{m2} &= 0.2\ \text{nM min}^{-1}, \\ k_u &= 0.4\ \text{min}^{-1}, \\ d_m &= 0.4\ \text{min}^{-1}, \\ s_p &= 1.4\ \text{nM min}^{-1}, \\ K_m &= 100\ \text{nM}, \\ d_p &= 2 \times 10^{-4}\ \text{min}^{-1}. \end{aligned} \tag{45}$$

For simplicity, we take the small function $S(t) \equiv 0$. The system has a unique steady state $(P_I^*, M^*, C^*, P_A^*) = (9.42094, 0.0372868, 3.49529, 0)$. The rate matrix Ω has the eigenvalues

$$\begin{aligned} \lambda_1 &= -38.4766, \\ \lambda_{2,3} &= -0.0028 \pm 0.0220i, \\ \lambda_4 &= -0.2002. \end{aligned} \tag{46}$$

Since all the eigenvalues have negative real parts, the steady state is asymptotically stable.

Figure 7(a) shows three solution trajectories projected on the inactive p53-complex plane starting at $(P_I(0), M_0(0), C_0(0), P_A(0)) = (5, 0.01, 0, 0), (30, 0.01, 0, 0), (15, 0.01, 0, 0)$, respectively. Figure 7(b) shows the time evolution of concentrations of p53 and mdm2.

With the values of parameters in (45) and initial data and initial values $P_I(0) = 10$, $M(0) = 0.1$, $C(0) = 3$, and $P_A(0) = 0$,8, we integrate system (25) on the time interval $[0, 100]$ by the methods expEuler, expHeun, expRK3/8, and expRK4 as well as their corresponding prototype methods with the step size $h = 1/16$. In Figures 8 and 9, we plot the global error growth of the inactive p53 on the time interval $[50, 100]$.

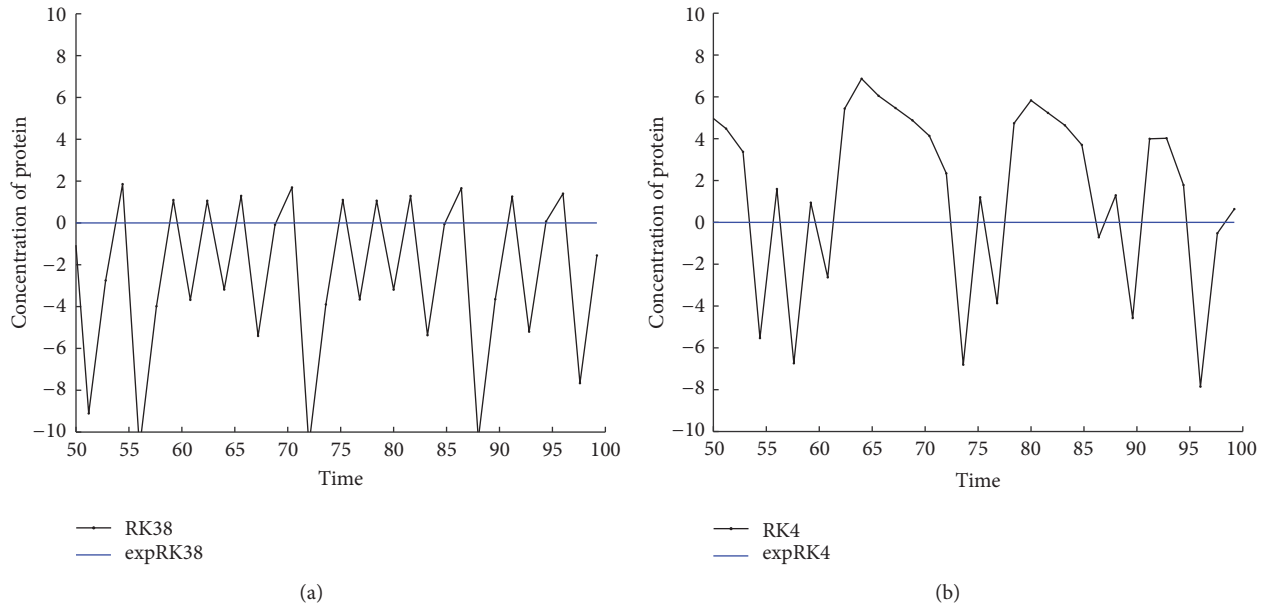

Figure 3: Accuracy comparison for the one-gene system: (a) RK3/8 and expRK3/8; (b) RK4 and expRK4 with step size $h = 1.6$.

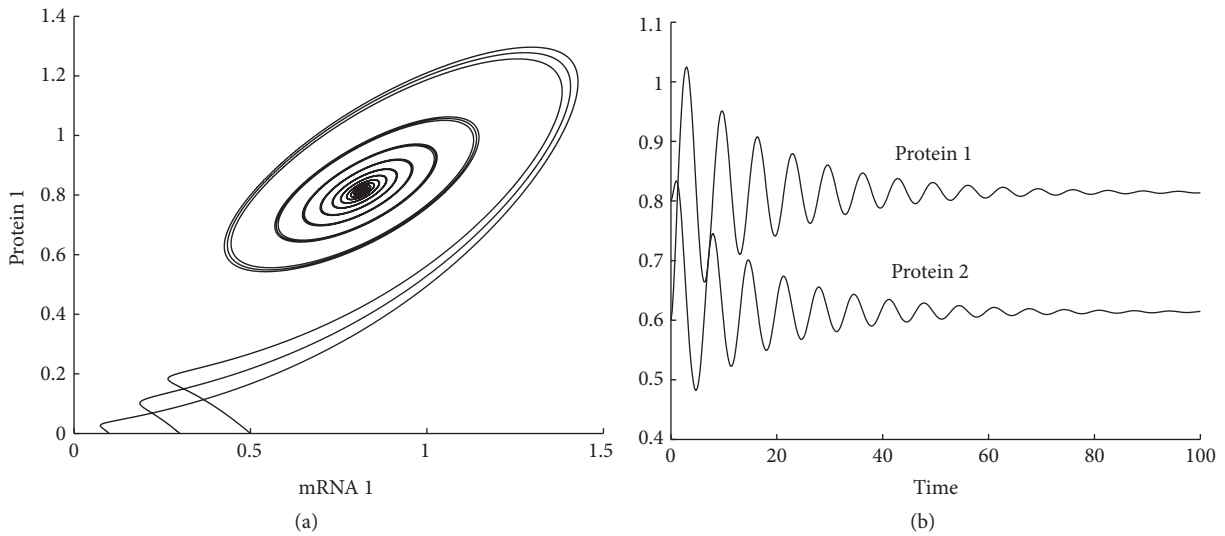

Figure 4: Two-gene system: (a) phase trajectories projected on mRNA 1-protein 1 plane; (b) time evolution of concentrations of proteins.

The problem is solved on the interval $[0, 50]$ for differential step sizes and the average errors are presented in Tables 5 and 6.

From Figures 2, 3, 5, 6, 8, and 9 and Tables 1–6, we can see that the new expRK methods expEuler, expHeun, expRK3/8, and expRK4 are much more accurate than their corresponding prototype methods.

3.2. Efficiency Test. In this subsection we will compare the simulation efficiency of the newly constructed exponential RK methods with some famous exponential integrators. The integrators we choose for comparison are listed as follows:

Table 1: One-gene system: comparison of average errors for Euler, expEuler, Heun, and expEuler methods.

Step size	Euler	expEuler	Heun	expHeun
1/4	3.5849×10^{-2}	1.1696×10^{-3}	2.1384×10^{-2}	1.5011×10^{-4}
1/8	2.6231×10^{-2}	5.2015×10^{-4}	2.0930×10^{-2}	5.7342×10^{-5}
1/16	2.2715×10^{-2}	2.3383×10^{-4}	2.0539×10^{-2}	3.8767×10^{-5}
1/32	2.1259×10^{-2}	9.8536×10^{-5}	2.0284×10^{-2}	3.5349×10^{-5}

(i) expRK3/8: the expRK method defined by (12) whose prototype RK method is given by (20)

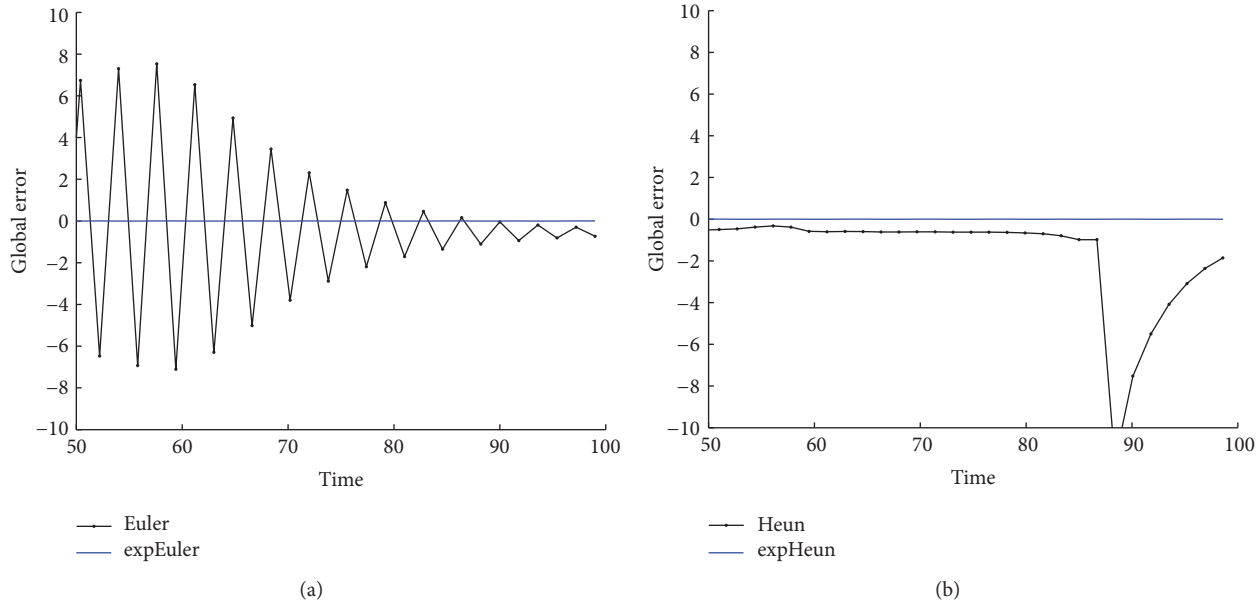

Figure 5: Accuracy comparison for the two-gene system: (a) Euler and expEuler; (b) Heun and expHeun.

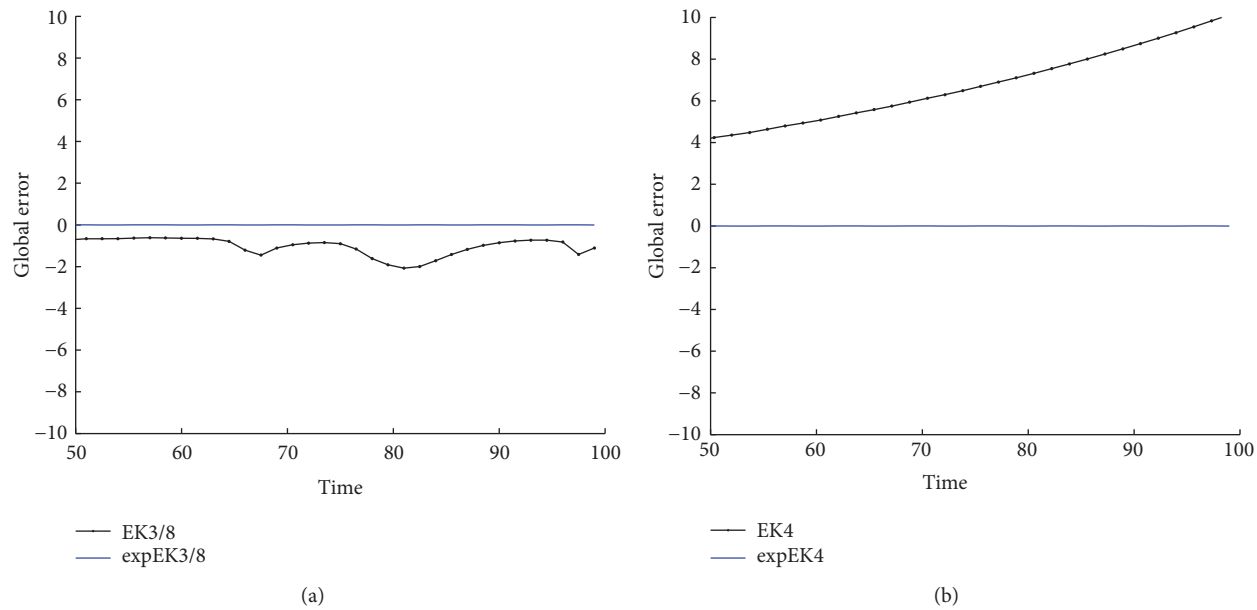

Figure 6: Accuracy comparison for the two-gene system: (a) RK3/8 and expRK3/8; (b) RK4 and expRK4.

(ii) expRK4: the expRK method defined by (12) whose prototype RK method is given by (21)

(iii) COX-MATTHEWS: the exponential RK method given by Cox and Matthews [34]

(iv) KROGSTAD: the exponential RK method given by Krogstad [35]

(v) STREHMEL-WEINER: the exponential RK method given by Strehmel [36] (Example 4.5.5)

(vi) HOCHBRUCK-OSTERMANN: the exponential RK method given by Hochbruck and Ostermann [23]

The criterion for the efficiency is the digital logarithm of the global error against the CPU-time consumed. System (25) with parameters (38) is solved on the time interval $[0, 100]$ with the step sizes $h = 1/2^j$, $j = 1, 2, 3, 4$. The numerical results are displayed in Figure 10, where we can see that the new exponential RK methods expEuler, expHeun, expRK3/8, and expRK4 are much more efficient than the other exponential RK methods we select from the literature. For the two-gene system, among all the exponent integrators we consider, expEuler, though the simplest, turns out to be the most efficient. It is also interesting to observe that as

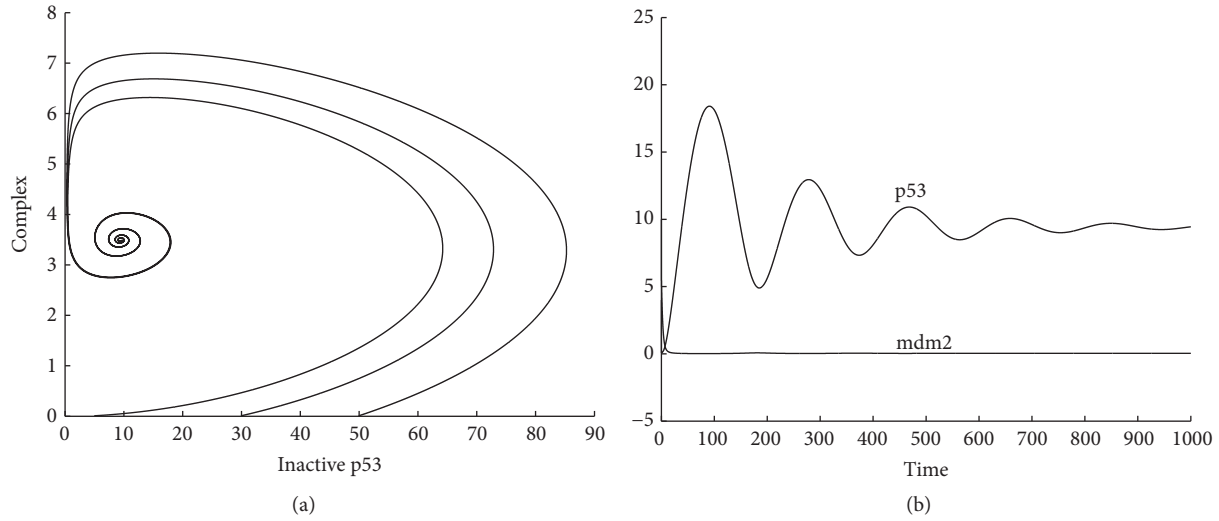

Figure 7: p53-mdm2 system: (a) phase curves projected on the inactive p53-complex plane; (b) time evolution of concentrations of p53 and mdm2.

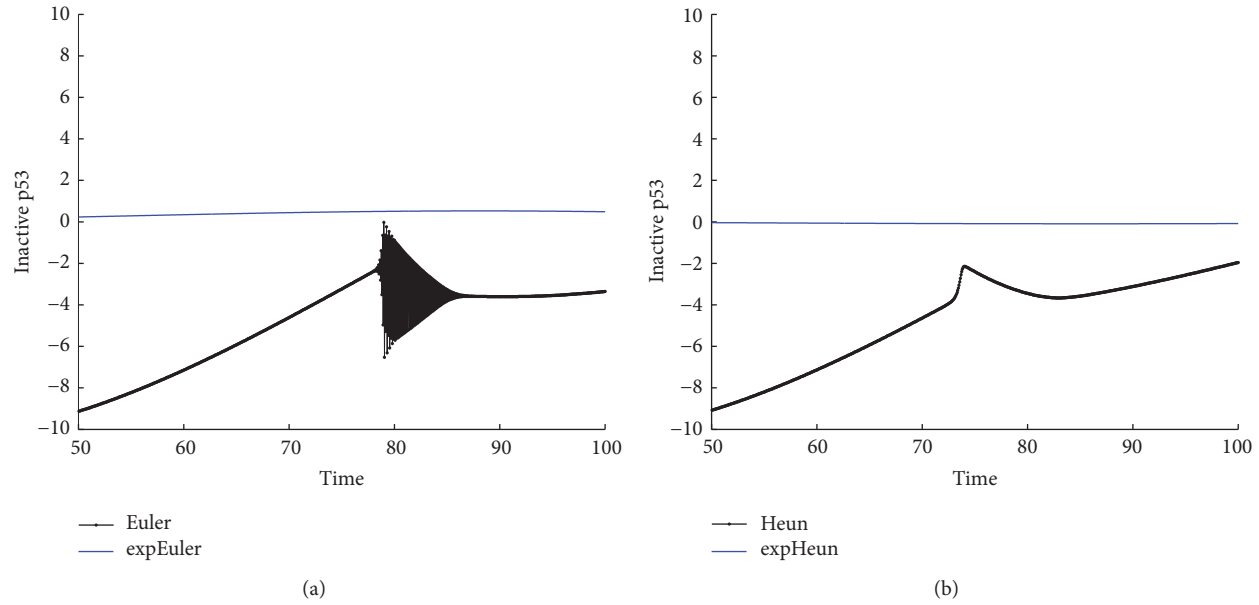

Figure 8: Accuracy comparison for the p53-mdm2 system: (a) Euler and expEuler; (b) Heun and expHeun.

integration step size decreases from $h = 1/2$, expRK4 cannot produce smaller error, just increasing the computation effort.

4. Conclusions and Discussions

Most genetic regulatory systems carry their own structures, such as stable steady states and sustained oscillation, bistability. Traditional Runge-Kutta (RK) methods have not taken into account these characteristic structures and may give misleading information. To see this, one only needs to integrate the two-gene system (25) by RK4 with step size $h = 1.32$. The simulation result, as presented in Figure 11, is qualitatively wrong. The exponential RK methods for system (3) originate from the discretization of the matrix form of variation-of-constants formula (8). This type of integrators has the property that they can integrate exactly linear systems of ODEs and thus can preserve the steady-state structure of

Table 2: One-gene system: comparison of average errors for RK3/8, expRK3/8, RK4, and expRK4 methods.

Step size	RK3/8	expRK3/8	RK4	expRK4
1/4	3.0743×10^{-2}	3.1270×10^{-5}	3.1713×10^{-2}	2.2006×10^{-4}
1/8	2.5309×10^{-2}	3.4131×10^{-5}	2.5490×10^{-2}	3.4655×10^{-5}
1/16	2.2533×10^{-2}	3.4373×10^{-5}	2.2569×10^{-2}	3.4403×10^{-5}
1/32	2.1219×10^{-2}	3.4407×10^{-5}	2.1227×10^{-2}	3.4408×10^{-5}

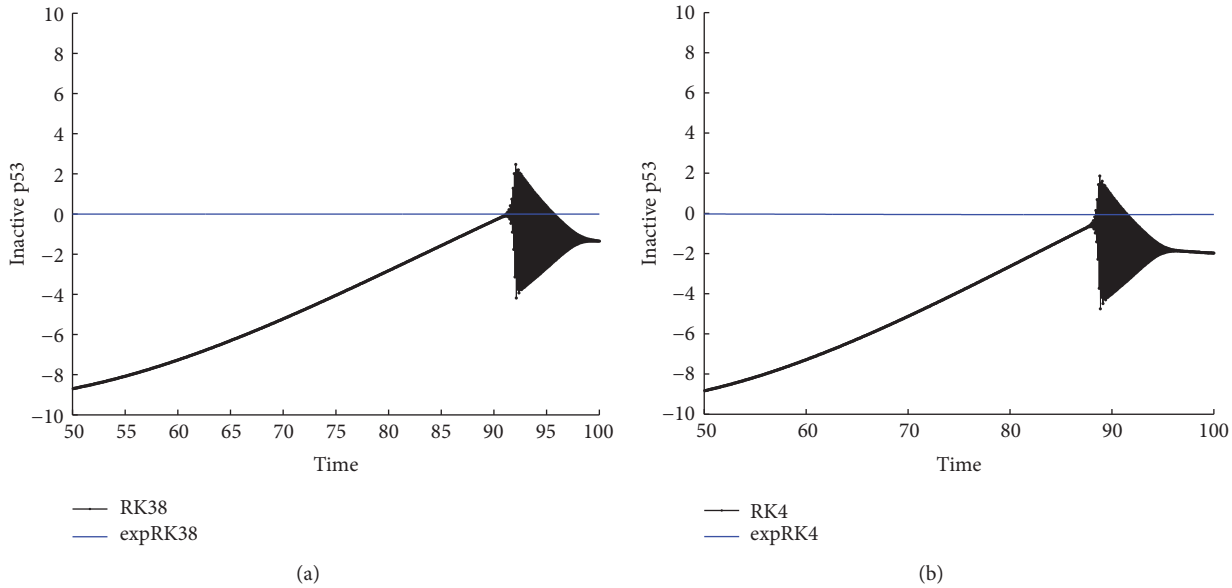

Figure 9: Accuracy comparison for the p53-mdm2 system: (a) RK3/8 and expRK3/8; (b) RK4 and expRK4.

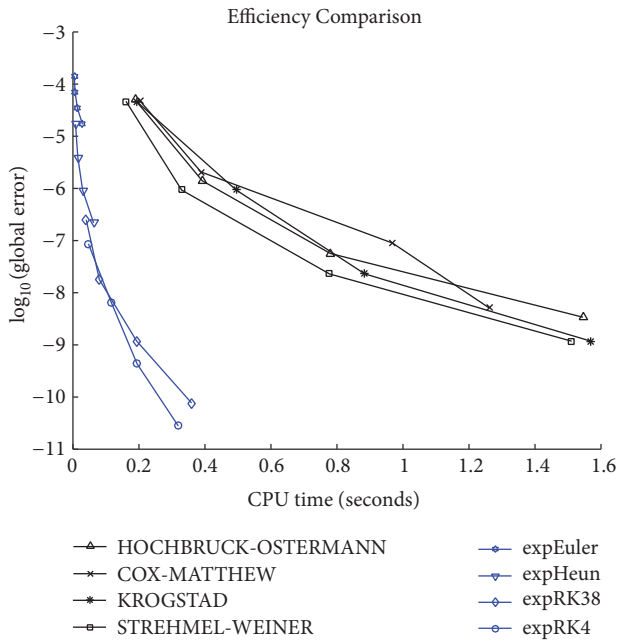

Figure 10: Efficiency curves with step sizes $h = 1/2^j$, $j = 1, 2, 3, 4$.

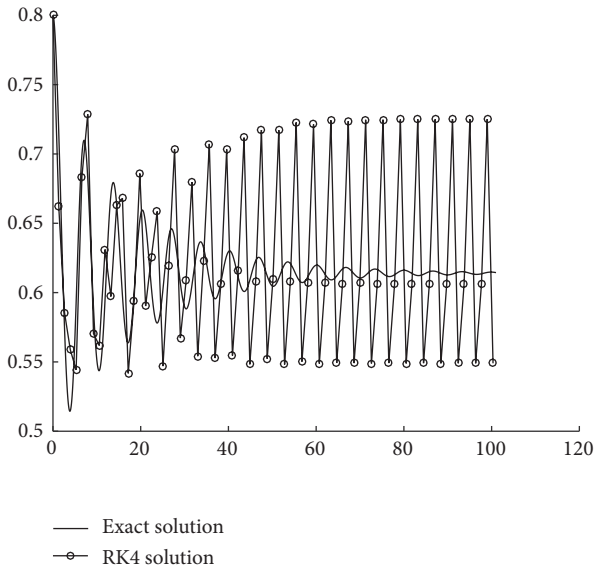

Figure 11: RK4 simulation with step size $h = 1.32$ compared with the exact solution.

system (3). From the numerical results presented in Section 3, an expRK method is more accurate than its traditional prototype RK method for long-term simulation with large step sizes. On the other hand, despite the simple form, the new expRK methods considered in this paper are tested to be more efficient than those prominent exponential RK methods when they are applied to genetic regulatory systems. The following advantages contribute to the high accuracy and high efficiency of the expRK methods compared to the classical RK methods.

(a) The scheme of the expRK methods recovers by the exponential functions the principal oscillatory structure of the true solution, which is contained in linear part (the Jacobian) of the system.

(b) The construction of the scheme is very simple and the coefficients are immediately obtained from a classical Runge-Kutta (RK) method.

(c) As shown in Appendix, the expRK methods (RK3/8 and RK4) have distortion and dissipation of the same order as their prototype RK methods but have dispersion of one order higher than their prototype RK methods. As the principal frequency is estimated accurately enough, that is, the ratio of

Table 3: Two-gene system: comparison of average errors for Euler, expEuler, Heun, and expHeun methods.

Step size	Euler	expEuler	Heun	expHeun
1	1.6832	4.4456×10^{-3}	2.9451×10^{-1}	2.1871×10^{-3}
1/2	9.21627×10^{-1}	2.4275×10^{-3}	4.0230×10^{-2}	1.0848×10^{-3}
1/4	5.1922×10^{-1}	1.4028×10^{-3}	1.0096×10^{-2}	9.5000×10^{-4}
1/8	1.8775×10^{-1}	1.0103×10^{-3}	2.7588×10^{-3}	9.4565×10^{-4}
1/16	5.0636×10^{-2}	9.0239×10^{-4}	1.1937×10^{-3}	9.4830×10^{-4}
1/32	1.8282×10^{-2}	8.9416×10^{-4}	9.8137×10^{-4}	9.4942×10^{-4}

Table 4: Two-gene system: comparison of average errors for RK3/8, expRK3/8, RK4, and expRK4 methods.

Step size	RK3/8	expRK3/8	RK4	expRK4
1	4.6619×10^{-2}	8.7331×10^{-4}	8.6240×10^{-3}	9.7906×10^{-4}
1/2	3.7028×10^{-1}	9.4577×10^{-4}	5.2468×10^{-1}	9.4457×10^{-4}
1/4	3.2666×10^{-1}	9.4805×10^{-4}	3.6973×10^{-1}	9.4766×10^{-4}
1/8	1.3398×10^{-1}	9.4894×10^{-4}	1.4412×10^{-1}	9.4891×10^{-4}
1/16	4.4359×10^{-2}	9.4947×10^{-4}	4.5572×10^{-2}	9.4947×10^{-4}
1/32	1.7338×10^{-2}	9.4974×10^{-4}	1.7525×10^{-2}	9.4974×10^{-4}

Table 5: p53-mdm2 system: comparison of average errors for Euler, expEuler, Heun, and expHeun methods.

Step size	Euler	expEuler	Heun	expHeun
1/16	3.5455	9.7152×10^{-3}	3.3784	2.47061×10^{-3}
1/32	1.3141×10^{-3}	5.3681×10^{-3}	1.7446×10^{-4}	1.2767×10^{-3}
1/64	6.5825×10^{-4}	2.7553×10^{-3}	5.9564×10^{-5}	4.383×10^{-4}
1/128	3.0970×10^{-4}	1.3769×10^{-3}	4.7031×10^{-5}	1.1482×10^{-4}

Table 6: p53-mdm2 system: comparison of average errors for RK3/8, expRK3/8, RK4, and expRK4 methods.

Step size	RK3/8	expRK3/8	RK4	expRK4
1/16	3.1651	2.2126×10^{-4}	3.2096	7.8709×10^{-4}
1/32	1.2676×10^{-3}	2.5953×10^{-5}	1.2770×10^{-3}	9.4086×10^{-5}
1/64	6.4492×10^{-4}	4.2016×10^{-5}	6.4759×10^{-4}	4.8393×10^{-5}
1/128	3.0628×10^{-4}	4.4244×10^{-5}	3.0697×10^{-4}	4.4697×10^{-5}

the error of estimation and the testing frequency $|r| \ll 1$, the coefficients of the leading terms of distortion and dissipation of the new expRK methods are much less than those of their prototype RK methods. Moreover, if ω is known to be the exact frequency ($r = 1$), expRK methods become zero-distortive, zero-dispersive, and zero-dissipative.

Although there may exist other methods of higher algebraic order that have higher accuracy, the expRK methods (12) are the most natural ones and are the most convenient to use. Note also that, similar to the approach of `ode45`, we can control the step by embedding two expRK methods of orders p and $p+1$ into a pair to achieve higher efficiency.

Indeed, the test problem (25) is assumed to be nonstiff and this may be why our expRK methods outperform the existing exponential Runge-Kutta methods of Cox and Matthews, Hochbruck and Ostermann, Krogstad, and Stehmel and Weiner. The consideration of expRK methods for stiff genetic regulatory system (such as the p53-mdm2 systems, whose Jacobian possesses eigenvalues with large negative real parts or with purely imaginary eigenvalues of large modulus) is an interesting theme for future work. These systems contain different time scales due to coexistence of fast reactions and slow reactions which are frequently encountered in real cell processes. The expRK methods adapted to stiff systems will have a more delicate scheme to incorporate the stiff structure.

Appendix

A. Proof of Theorem 4

A fixed point of scheme (12) is a point y^* such that $y_n = y^*$ implies $y_{n+1} = y^*$. We have assumed that $f(0) = 0$. Suppose that $y_n = 0$ in scheme (12). The internal stages of scheme (12) define a nonlinear operator $\Psi : Y \mapsto \Psi(Y)$ on $\mathbb{R}^{sd}$. For $Y, Z \in \mathbb{R}^{sd}$, the internal stages of system (12) are

$$\begin{aligned}
\|\mathscr{L}(Y) - \mathscr{L}(Z)\| &= \Bigg\| h \Bigg(\sum_{j=1}^{s} a_{1j} \exp\left(\left(c_1 - c_j\right) V\right) \\
&\cdot \left(f\left(Y_j\right) - f\left(Z_j\right) - \Omega\left(Y_j - Z_j\right)\right), \ldots, \sum_{j=1}^{s} a_{sj} \\
&\cdot \exp\left(\left(c_s - c_j\right) V\right) \\
&\cdot \left(f\left(Y_j\right) - f\left(Z_j\right) - \Omega\left(Y_j - Z_j\right)\right) \Bigg)^T \Bigg\| \\
&\leq h \sum_{i,j=1}^{s} \left|a_{ij}\right| \cdot \left\|\exp\left(\left(c_i - c_j\right) V\right)\right\| \cdot \left(\left\|f\left(Y_j\right)\right.\right. \\
&\left.\left. - f\left(Z_j\right)\right\| + \|\Omega\| \cdot \left\|Y_j - Z_j\right\|\right) \leq h \sum_{i,j=1}^{s} \left|a_{ij}\right| \\
&\cdot \left\|\exp\left(\left(c_i - c_j\right) V\right)\right\| \cdot (L + \|\Omega\|) \left\|Y_j - Z_j\right\| \\
&\leq h \sum_{i,j=1}^{s} \left|a_{ij}\right| \cdot \left\|\exp\left(\left(c_i - c_j\right) V\right)\right\| \cdot (L + \|\Omega\|) \cdot \|Y \\
&- Z\| = L_1 \|Y - Z\|,
\end{aligned} \tag{A.1}$$

where $L_1 = h \sum_{i,j=1}^{s} |a_{ij}| \cdot \| \exp((c_i - c_j)V)\|(L + \|\Omega\|) < 1$ if $h < 1/\sum_{i,j=1}^{s} |a_{ij}| \cdot \|\exp((c_i - c_j)V)\| \cdot (L + \|\Omega\|)$. Therefore, Ψ is a contraction on $\mathbb{R}^{sd}$. By the *Banach contraction theorem*, the operator Ψ has a unique fixed point $Y = 0$; that is, $Y_i = 0$ for $i = 1, \ldots, s$ which implies that $y_{n+1} = 0$. We have proven that the origin $y^* = 0$ is the unique fixed point of the exponential RK method (12).

B. Analysis of Linear Stability, Distortion, Dispersion, and Dissipation

In this section, in order to examine the behavior of an RK or expRK method $\Phi_h : y_n \to y_{n+1}$ for the dynamical system defined by ODE (3) with a stable steady state $y^* = 0$, we analyze its linear stability and estimate the orders of distortion, dispersion, and dissipation.

Let us consider the linear scalar test equation

$$\dot{y} - \Omega y = \varepsilon y, \tag{B.1}$$

where the complex number Ω is an estimate of the principal rate and ε is the error of the estimation. Applying an RK method (5) or an expRK method (12) to (B.1) yields

$$y_{n+1} = R(V, z)\, y_n, \quad V = h\Omega,\ z = h\varepsilon, \tag{B.2}$$

where $R(V, z)$ is called the *stability function* of the method.

For an s-stage RK method,

$$R(V, z) = 1 + Hb^T \left(I_s - HA\right)^{-1} e, \quad H = V + z, \tag{B.3}$$

where I_s is the $d \times d$ identity matrix and the s-dimensional vector $e = (1, \ldots, 1)^T$. For an explicit s-stage RK method, since the matrix A is an $s \times s$ lower-triangular, then $A^s = 0$ and

$$\begin{aligned} R(V, z) = 1 + Hb^T e - H^2 b^T A e + \cdots \\ + (-1)^{s-1} H^{s-1} b^T A^{s-1} e. \end{aligned} \tag{B.4}$$

On the other hand, an s-stage expRK method (12) has a distortion

$$R(V, z) = \exp(V) + z \exp(V)\, b(V)^T \left(I_s - zA\right)^{-1} e. \tag{B.5}$$

If the expRK method is explicit,

$$\begin{aligned} R(V, z) = \exp(V) \Big(1 + zb(V)^T e - z^2 b(V)^T A e + \cdots \\ + (-1)^{s-1} z^s b(V)^T A^{s-1} e\Big). \end{aligned} \tag{B.6}$$

Definition B.1. For an s-stage method with the stability function $R(V, z)$, the region in the (V, z) plane

$$\mathcal{R}_s = \{(V, z) \mid |R(V, z)| \le 1\} \tag{B.7}$$

is called the *stability region* of the method.

Figure 12 presents the stability regions of RK4 (left) and expRK4, respectively.

Definition B.2. For an s-stage expRK method (5) with the stability function $R(V, z)$, the quantity

$$\mathrm{Dist}(H) = H - \ln R(V, z), \quad H = V + z \tag{B.8}$$

is called the *distortion* (or *rate error*) of the method. If $\mathrm{Dist}(H) = \mathcal{O}(H^{k+1})$ as $H \to 0$, then the method is called *distortive of order k*. If $\mathrm{Dist}(H) = 0$, then the method is called *zero-distortive*.

The distortion of RK4 method is

$$\mathrm{Dist}(H) = \frac{1}{120} H^5 - \frac{1}{144} H^6 + \mathcal{O}\left(H^7\right), \quad H \longrightarrow 0. \tag{B.9}$$

On the other hand, if we denote the ratio $r = \varepsilon/\Omega = z/V$, then $V = (1/(1 + r))H$ and $z = (r/(1 + r))H$ and the distortion of the expRK4 method is

$$\begin{aligned} \mathrm{Dist}(H) = \frac{r^5}{120(1 + r)^5} H^5 - \frac{r^6}{144(1 + r)^6} H^6 \\ + \mathcal{O}\left(H^7\right), \quad H \longrightarrow 0. \end{aligned} \tag{B.10}$$

It can be seen from (B.9) and (B.10) that RK4 and expRK4 are both distortive of order four. However, if an estimate ε of the true rate Ω is accurate enough, that is, $|r| \ll 1$, then the coefficient of the leading term of the distortion $\mathrm{Dist}(H)$ for the expRK4 method is much smaller than that for the RK method. Moreover, if the frequency can be estimated exactly ($r = 1$), then all the expRK methods are zero-distortive.

It has been observed that most genetic regulatory systems have oscillatory solutions. Therefore it is of importance to measure to what extent a numerical method can preserve the oscillation. In order to compare the accuracy RK methods and that of expRK methods in preserving the oscillatory properties of the exact solution, we assume that Ω and ε in the test equation (B.1) are purely imaginary; that is, $\Omega = i\lambda$, $\varepsilon = i\mu$, $i^2 = -1$.

Definition B.3. For a method with stability function $R(V, z)$, denote the real and imaginary parts of the stability function $R(V, z)$ by $U(V, z)$ and $Q(V, z)$, respectively, where $\xi = h\lambda$ and $\eta = h\mu$. The quantities

$$\begin{aligned} \mathrm{Disp}(\theta) = \theta - \arccos \frac{Q(\xi, \eta)}{\sqrt{U^2(\xi, \eta) + Q^2(\xi, \eta)}}, \\ \mathrm{Dis}(\theta) = 1 - \sqrt{U^2(\xi, \eta) + Q^2(\xi, \eta)}, \quad \theta = \xi + \eta, \end{aligned} \tag{B.11}$$

are called the *dispersion* (or *phase lag*) and *dissipation* (or *amplification factor error*) of the method, respectively. If $\mathrm{Disp}(\theta) = \mathcal{O}(\theta^{q+1})$ and $\mathrm{Dis}(\theta) = \mathcal{O}(\theta^{l+1})$ as $\theta \to 0$, then the method is called *dispersive of order q* and *dissipative of order l*, respectively. If $\mathrm{Disp}(\theta) = 0$ and $\mathrm{Dis}(\theta) = 0$, then the method is called *zero-dispersive* and *zero-dissipative*, respectively.

For both RK4 and RK3/8, the dispersion and dissipation satisfy

$$\begin{aligned} \mathrm{Disp}(\theta) = -\frac{\theta^5}{120} + \mathcal{O}\left(\theta^7\right), \\ \mathrm{Dis}(\theta) = \frac{\theta^6}{144} + \mathcal{O}\left(\theta^8\right). \end{aligned} \tag{B.12}$$

Therefore, RK4 and RK3/8 both are dispersive of order four and dissipative of order five.

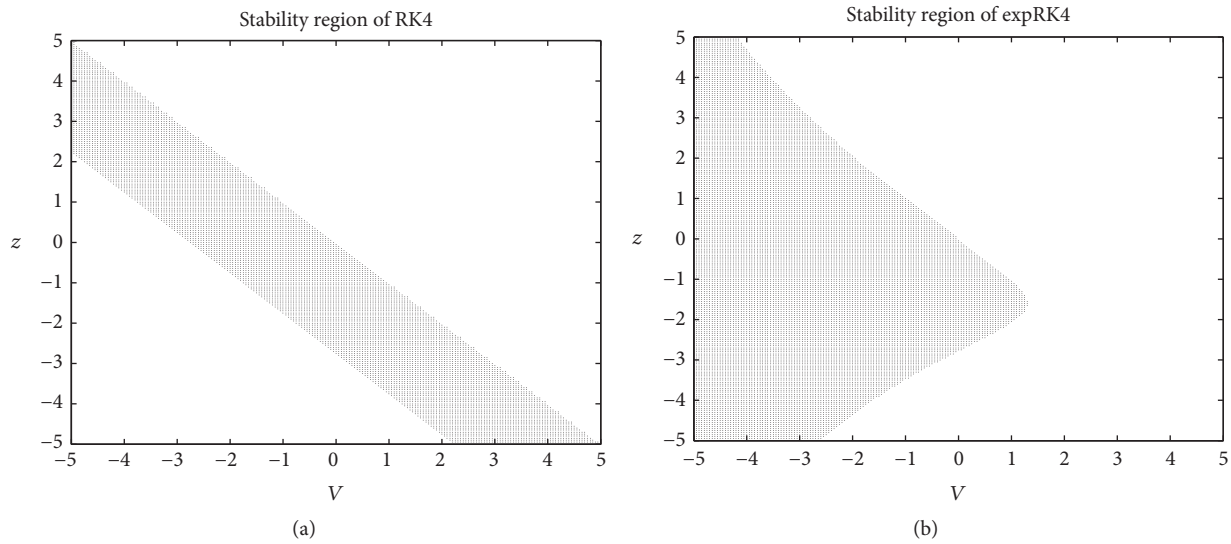

Figure 12: (a) Stability region of RK4; (b) stability region of expRK4.

Let $r = \mu/\lambda$. Then the dispersion and dissipation for both expRK4 and expRK3/8 are

$$\begin{aligned} \text{Disp}(\theta) &= -\frac{r^5\left(1+3r+r^2\right)}{120\,(1+r)^6}\theta^6 + \mathcal{O}\left(\theta^8\right), \\ \text{Dis}(\theta) &= \frac{r^6}{144\,(1+r)^6}\theta^6 + \mathcal{O}\left(\theta^8\right), \\ &\theta \longrightarrow 0. \end{aligned} \tag{B.13}$$

Therefore, expRK4 and expRK3/8 both are dispersive of order five and dissipative of order five. Then expRK4 (expRK3/8) has dispersion of one order higher than RK4 (RK3/8). If $|r| \ll 1$, then the coefficient of the leading term of the dissipation Diss(θ) for the expRK4 (expRK3/8) method is much smaller than that for RK4 (RK3/8). Furthermore, if $r = 1$, then all the expRK methods are zero-dispersive and zero-dissipative.

The above analysis explains why, when the rate Ω of the problem is estimated accurately enough, an expRK method is more accurate than its prototype RK method in preserving the distortion, dispersion, and dissipation of the exact solution.

Competing Interests

The authors declare that there is no conflict of interests regarding the publication of this paper.

Acknowledgments

This research was partially supported by the National Natural Science Foundation of China (NSFC) (Grant no. 11171155), the State Key Program of Natural Science Foundation of China (Grant no. 31330067), and the Fundamental Research Fund for the Central Universities (Grant no. KYZ201424).

References

[1] M. W. Kirschner, "The meaning of systems biology," *Cell*, vol. 121, no. 4, pp. 503–504, 2005.

[2] H. Kitano, "Systems biology: a brief overview," *Science*, vol. 295, no. 5560, pp. 1662–1664, 2002.

[3] M. B. Elowitz and S. Leibier, "A synthetic oscillatory network of transcriptional regulators," *Nature*, vol. 403, no. 6767, pp. 335–338, 2000.

[4] T. S. Gardner, C. R. Cantor, and J. J. Collins, "Construction of a genetic toggle switch in *Escherichia coli*," *Nature*, vol. 403, no. 6767, pp. 339–342, 2000.

[5] E. M. Ozbudak, M. Thattal, H. H. Lim, B. I. Shraiman, and A. Van Oudenaarden, "Multistability in the lactose utilization network of Escherichia coli," *Nature*, vol. 427, no. 6976, pp. 737–740, 2004.

[6] R. Weiss, T. Knight, and G. Sussman Jr., "Cellular computation and communication using engineered genetic regulatory networks," in *Cellular Computing*, M. Amos, Ed., Oxford University Press, Oxford, UK, 2004.

[7] P. Smolen, D. A. Baxter, and J. H. Byrne, "Mathematical modeling of gene networks," *Neuron*, vol. 26, no. 3, pp. 567–580, 2000.

[8] B. C. Goodwin, "Oscillatory behavior in enzymatic control processes," *Advances in Enzyme Regulation*, vol. 3, pp. 425–439, 1965.

[9] R. Thomas and R. D'Ari, *Biological Feedback*, CRC Press, 1990.

[10] C. P. Fall, E. S. Marland, J. M. Wagner, and J. J. Tyson, *Computational Cell Biology*, Springer, 2002.

[11] K. Iwamoto, H. Hamada, Y. Eguchi, and M. Okamoto, "Mathematical modeling of cell cycle regulation in response to DNA damage: exploring mechanisms of cell-fate determination," *BioSystems*, vol. 103, no. 3, pp. 384–391, 2011.

[12] A. Altinok, D. Gonze, F. Lévi, and A. Goldbeter, "An automaton model for the cell cycle," *Interface Focus*, vol. 1, no. 1, pp. 36–47, 2011.

[13] C. Gérard and A. Goldbeter, "A skeleton model for the network of cyclin-dependent kinases driving the mammalian cell cycle," *Interface Focus*, vol. 1, no. 1, pp. 24–35, 2011.

[14] A. Goldbeter, "Oscillatory enzyme reactions and Michaelis-Menten kinetics," *FEBS Letters*, vol. 587, no. 17, pp. 2778–2784, 2013.

[15] A. Polynikis, S. J. Hogan, and M. di Bernardo, "Comparing different ODE modelling approaches for gene regulatory networks," *Journal of Theoretical Biology*, vol. 261, no. 4, pp. 511–530, 2009.

[16] R. Thomas, D. Thieffry, and M. Kaufman, "Dynamical behaviour of biological regulatory networks-I. Biological role of feedback loops and practical use of the concept of the loop-characteristic state," *Bulletin of Mathematical Biology*, vol. 57, no. 2, pp. 247–276, 1995.

[17] S. Widder, J. Schicho, and P. Schuster, "Dynamic patterns of gene regulation I: simple two-gene systems," *Journal of Theoretical Biology*, vol. 246, no. 3, pp. 395–419, 2007.

[18] H. Shinto, Y. Tashiro, M. Yamashita et al., "Kinetic modeling and sensitivity analysis of acetone-butanol-ethanol production," *Journal of Biotechnology*, vol. 131, no. 1, pp. 45–56, 2007.

[19] E. Hairer, S. P. Nørsett, and G. Wanner, *Solving ordinary differential equations I*, vol. 8 of *Springer Series in Computational Mathematics*, Springer, Berlin, Germany, Second edition, 1993.

[20] A. M. Stuart and A. R. Humphries, *Dynamical Systems and Numerical Analysis*, Cambridge University Press, 1995.

[21] E. Hairer, C. Lubich, and G. Wanner, *Geometric Numerical Integration*, vol. 31 of *Springer Series in Computational Mathematics*, Springer, Berlin, Germany, 2nd edition, 2006.

[22] X. Wu, X. You, and B. Wang, *Structure-preserving algorithms for oscillatory differential equations*, Springer Berlin Heidelberg, 2013.

[23] M. Hochbruck and A. Ostermann, "Explicit exponential Runge-Kutta methods for semilinear parabolic problems," *SIAM Journal on Numerical Analysis*, vol. 43, no. 3, pp. 1069–1090, 2005.

[24] O. Defterlia, A. Fügenschuhb, and G. W. Weberc, "Modern tools for the time-discrete dynamics and optimization of gene-environment networks," *Communications in Nonlinear Science and Numerical Simulation*, vol. 16, no. 12, pp. 4768–4779, 2011.

[25] G. W. Weber, O. Defterli, S. Z. Alparslan Gök, and E. Kropat, "Modeling, inference and optimization of regulatory networks based on time series data," *European Journal of Operational Research*, vol. 211, no. 1, pp. 1–14, 2011.

[26] X. You, "Limit-cycle-preserving simulation of gene regulatory oscillators," *Discrete Dynamics in Nature and Society*, vol. 2012, Article ID 673296, 22 pages, 2012.

[27] X. You, X. Liu, and I. H. Musa, "Splitting strategy for simulating genetic regulatory networks," *Computational and Mathematical Methods in Medicine*, vol. 2014, Article ID 683235, 9 pages, 2014.

[28] Z. Chen, J. Li, R. Zhang, and X. You, "Exponentially fitted two-derivative Runge-Kutta methods for simulation of oscillatory genetic regulatory systems," *Computational and Mathematical Methods in Medicine*, vol. 2015, Article ID 689137, 14 pages, 2015.

[29] R. Zhang, W. Jiang, J. O. Ehigie, Y. Fang, and X. You, "Novel phase-fitted symmetric splitting methods for chemical oscillators," *Journal of Mathematical Chemistry*, pp. 1–21, 2016.

[30] M. W. Hirsch, S. Smale, and R. L. Devaney, *Differential Equations, Dynamical Systems, and An Introduction to Chaos*, Academic Press, 2013.

[31] M. Xiao and J. Cao, "Genetic oscillation deduced from Hopf bifurcation in a genetic regulatory network with delays," *Mathematical Biosciences*, vol. 215, no. 1, pp. 55–63, 2008.

[32] Z. Chen, X. You, X. Shu, and M. Zhang, "A new family of phase-fitted and amplification-fitted Runge-Kutta type methods for oscillators," *Journal of Applied Mathematics*, vol. 2012, Article ID 236281, 27 pages, 2012.

[33] I. M. M. van Leeuwen, I. Sanders, O. Staples, S. Lain, and A. J. Munro, "Numerical and experimental analysis of the p53-mdm2 regulatory pathway," in *Digital Ecosystems: Third International Conference, OPAALS 2010, Aracuju, Sergipe, Brazil, March 22-23, 2010, Revised Selected Papers*, F. A. B. Colugnati, L. C. R. Lopes, and S. F. A. Barretto, Eds., vol. 67 of *Lecture Notes of the Institute for Computer Sciences, Social Informatics and Telecommunications Engineering*, pp. 266–284, Springer, Berlin, Germany, 2010.

[34] S. M. Cox and P. C. Matthews, "Exponential time differencing for stiff systems," *Journal of Computational Physics*, vol. 176, no. 2, pp. 430–455, 2002.

[35] S. Krogstad, "Generalized integrating factor methods for stiff PDEs," *Journal of Computational Physics*, vol. 203, no. 1, pp. 72–88, 2005.

[36] K. R. Strehmel, *Linear-Implizite Runge-Kutta Methoden und Ihre Anwendungen*, vol. 127 of *Teubner-Texte zur Mathematik*, Teubner, 1992.